

Comparison of Colorectal Cancer in Differentially Established Liver Metastasis Models

WOO YONG LEE^{1,2*}, HYE KYUNG HONG^{1*}, SOO KYUNG HAM¹, CHANG IN KIM¹ and YONG BEOM CHO^{1,2}

¹Department of Surgery, Samsung Medical Center,

Sungkyunkwan University School of Medicine, Gangnam-gu, Seoul, Republic of Korea;

²Department of Health Sciences and Technology, Samsung Advanced Institute for Health Sciences and Technology, Sungkyunkwan University, Seoul, Republic of Korea

Abstract. *Background:* Metastasis is one of the main reasons for colorectal cancer (CRC)-related deaths due to the lack of effective therapeutics mainly for liver metastasis. In the present study, we established an orthotopic colorectal cancer mouse model using different transplantation protocols to determine the optimal conditions for CRC liver metastasis. *Materials and Methods:* Luciferin-expressing HCT116 cells were used to induce liver metastasis models of colorectal cancer following both intra-splenic and cecal injections. Magnetic resonance imaging (MRI) and the In Vivo Imaging system were used to monitor internal growth of the primary tumor and metastasis. *Results:* The intra-splenic injection with high cell number (5×10^6 cells/50 μ L)-group achieved rapid tumor formation, and the highest metastatic rate. However, survival rates were shorter than those of the other groups. The time to develop primary tumors and liver metastases was slightly different between the two transplantation protocols followed and should be considered depending on the specific aim of each experiment. MRI and optical images correlated well with the pathological findings at necropsy with respect to both tumor growth and location. *Conclusion:* The model described herein will be effective in studying new therapeutic strategies against metastatic disease when used in conjunction with small animal MRI and optical imaging.

Colorectal cancer (CRC) is rated as the third and fourth most common cancer for females and males worldwide (1). CRC

*These Authors contributed equally to this work.

Correspondence to: Dr. Yong Beom Cho, Associate professor, Department of Surgery, Samsung Medical Center, Sungkyunkwan University School of Medicine, 81 Irwon-ro, Gangnam-gu, Seoul 135-710, Korea. Tel: +82 234101669, Fax: +82 234106980, e-mail: gscyb@skku.edu

Key Words: Liver metastasis, orthotopic model, cecal injection, intra-splenic injection.

is the second cause of cancer-related death for males and the third cause for females in developed countries (2). Metastasis is one of the main reasons for CRC-related death, and patients diagnosed with metastasis show a poor prognosis. Therefore, investigating the mechanism of liver metastasis and improving treatment are important to increase the survival rate of colorectal cancer.

A number of CRC animal models have been developed to evaluate the characteristics of CRC progression and its mechanism of liver metastases (3-5). These include chemically-induced models (6), genetically-engineered mouse models (7-9), and spontaneous-transplantable animal models (10-12). Although these models have been extremely useful for investigating CRC characteristics, the number of models is limited to a low metastatic tumor take-rate and restricted dissemination to the lymph nodes or lungs. Spontaneous implantation models are the model of choice to study metastatic mechanisms of human cancer (13). An animal model that fulfills the mechanism of metastasis would be a working model to evaluate new drug responses and to study the characteristics of molecular targeting involving the metastatic process.

In the present study, we used HCT116 cells expressing GFP-Luciferin to establish primary tumors and metastasis using intra-splenic and cecal injection transplantation methods with high and low cell numbers. Additionally, internal growth of the primary tumor and metastasis were monitored using optical imaging and magnetic resonance imaging (MRI) to determine the optimal conditions for this CRC liver metastasis model.

Materials and Methods

Animals. Six- to 8-week-old female BALB/c nu/nu mice weighing 15-18 g at the time of surgery were used. The mice were obtained from Orient Bio Group (Seoul, Korea), and maintained under specific pathogen-free conditions. All *in vivo* studies were performed in accordance with the institutional guidelines and were approved by the Institutional Animal Care and Use Committee (20130828002).

Cell culture and lentiviral transduction. The HCT116 cell line was obtained from the Korean Cell Line Bank (Seoul, Korea) and cultured in McCoy's 5A medium with 10% (v/v) fetal bovine serum (Gibco, Grand Island, NY, USA) and 1% (v/v) penicillin-streptomycin (Gibco). The cells were maintained in a 5% CO₂ incubator at 37°C. GFP-Luciferin lentivirus was added to the HCT116 cells (5×10⁴ cells/well in a 12-well plate) with 8 µg/mL Polybrene in media. After a 24-h incubation, the transduced cells were selected with 1000 µg/mL of hygromycin (Sigma, St. Louis, MO, USA). The selected HCT116-GFP-Luc cells were maintained in a 5% CO₂ incubator at 37°C in McCoy's 5A medium with 10% (v/v) fetal bovine serum, 1% (v/v) penicillin-streptomycin (Gibco), and 500 µg/mL hygromycin.

Intra-splenic and cecal injections. Nude mice were anesthetized with a mixture of Zoletil (30 mg/kg) and Rompun (10 mg/kg) by intra-peritoneal injection (0.01 mL/mg). The HCT116-GFP-Luc cells were prepared in low and high volume cell groups such as 2×10⁶ and 5×10⁶ cells/50 µL HBSS (Gibco) in one injection. A small left abdominal flank incision was made and the spleen was exteriorized for the intra-splenic injection. The prepared cells were injected into the spleen with a 30-gauge needle. To prevent tumor cell leakage and bleeding, a cotton swab was held over the site of injection for 1 min. The injected spleen was returned to the abdomen and the wound was sutured with 6-0 black silk. An incision was made on the middle of the lower abdomen for the cecal injection. The cecum was picked-out, and the prepared cells were injected with a 30-gauge needle. After the injection, the cecum was returned to the abdominal cavity, and the wound was closed as described previously.

Hematoxylin and eosin (H&E) staining. Five µm thick sections were cut from paraffin-embedded blocks using a microtome, deparaffinized in xylene, and rehydrated in an ethanol series and PBS. The sections were stained with H&E to examine tumor morphology.

Imaging. One week after the injection, we imaged the mouse model twice per week to monitor liver metastasis with the *In Vivo* Imaging System (IVIS Spectrum, Caliper, Hopkinton, MA, USA). MRI imaging (Biospec 7T, Bruker, Fullerton, CA, USA) was initiated 14 days after cell injection and repeated every 1 week for as long as the liver metastasis was detected. T2-weighted axial MRI sections were obtained in the following settings: fast spin echo sequence with time to repetition of 1143.8 msec and time to echo of 25.8 msec; 160×170 matrix; 24.0 mm × 26.0 mm field of view, signal averaging, 12; section thickness, 1.0 mm; gap, 0 mm. Bioluminescence imaging was obtained using the *In Vivo* Imaging System (IVIS Spectrum, Caliper, Hopkinton, MA, USA). Mice were injected with D-luciferin (150 mg/kg) intraperitoneally 5 min before imaging, anesthetized (1-2% isoflurane), and placed in a light-tight camera box on the stage of the imaging chamber. Mice were imaged for 1 min with sequential 5 sec exposures. Luminescence was quantified using the Living Image software 3.2 (Caliper).

Results

Tumorigenesis by intra-splenic injection. Carefully counted HCT116 cells were divided into two groups according to cell number such as 2×10⁶ (low-cell number group) and 5×10⁶ (high-cell number group) cells per injection. Eight nude mice

were used in each group. Notably, three mice in the high-cell number-injected group died unexpectedly within 7 days. Tumors had developed at the primary and hepatic sites in both groups. Interestingly, more lymph node metastases and peritoneal seeding were found in the low-cell number group (Figure 1A) (Table I). Both groups demonstrated 100% liver metastasis (8/8 in the low-cell number and 5/5 in the high-cell number groups), as determined by gross necropsy and histological examination (Table I). However, the phenotypes of the metastatic tumors were different. The metastatic tumor formed on a specific spot on the liver in the low-cell number intra-splenic injected group. However, the tumor spread out and almost covered the entire liver in the high-cell number intra-splenic injected group (Figure 1A and B). Based on the tumorigenesis rates and the shapes of the metastases, we used IVIS and MRI to compare the tumors in the abdomen between the two groups. Primary tumors were detected in both groups after 7 days (Figure 2). Liver metastasis appeared 25 days after the injection in the low-cell number intra-spleen injected group (Figure 3A and B). When we compared IVIS imaging 14 days after injection, we noticed that the high cell number group had faster tumor formation rates than those in the low cell number group of the intra-splenic injected mice (Figure 3C). MRI revealed liver metastases in all mice in the high-cell number group (Figure 3D).

Tumorigenesis by cecal injection. The 2×10⁶ and 5×10⁶ cell per injection groups had eight nude mice each. A primary tumor was detected in 7/8 mice when the low-cell number group was injected in the cecum, and 4/7 (57%) had a liver metastasis (Figure 4A) (Table II). The high-cell number cecal-injected group demonstrated an 8/8 (100%) tumor formation rate at the primary site and 6/8 (75%) liver metastases (Figure 4B) (Table II). The metastatic tumors formed on a specific spot in the liver in the low-cell number intra-splenic injected group (Figure 4A and B). Both groups showed lymph node metastases and peritoneal seeding (Table II). IVIS imaging 15 days after injection indicated distinct blue spots on the abdomen besides the primary site in the high-cell number cecal-injected group mice (Figure 5). However, no tumor was detected on MRI 15 days after injection (data not shown). Liver metastasis was detected 25 days after injection in the high-cell number group (Figure 6C and D) and 32 days after in the low-cell number group (Figure 6A and B).

Histological study of tumor invasiveness. We collected the primary and metastatic tumor tissues and studied tissue histology to investigate characteristic differences between the tumors of the intra-splenic and cecal-injected groups (Figure 7). The tumor cells had broken through the epithelial cells and were located within the muscle layer. The primary tumor invaded in both groups, and their liver metastases were shown with H&E staining.

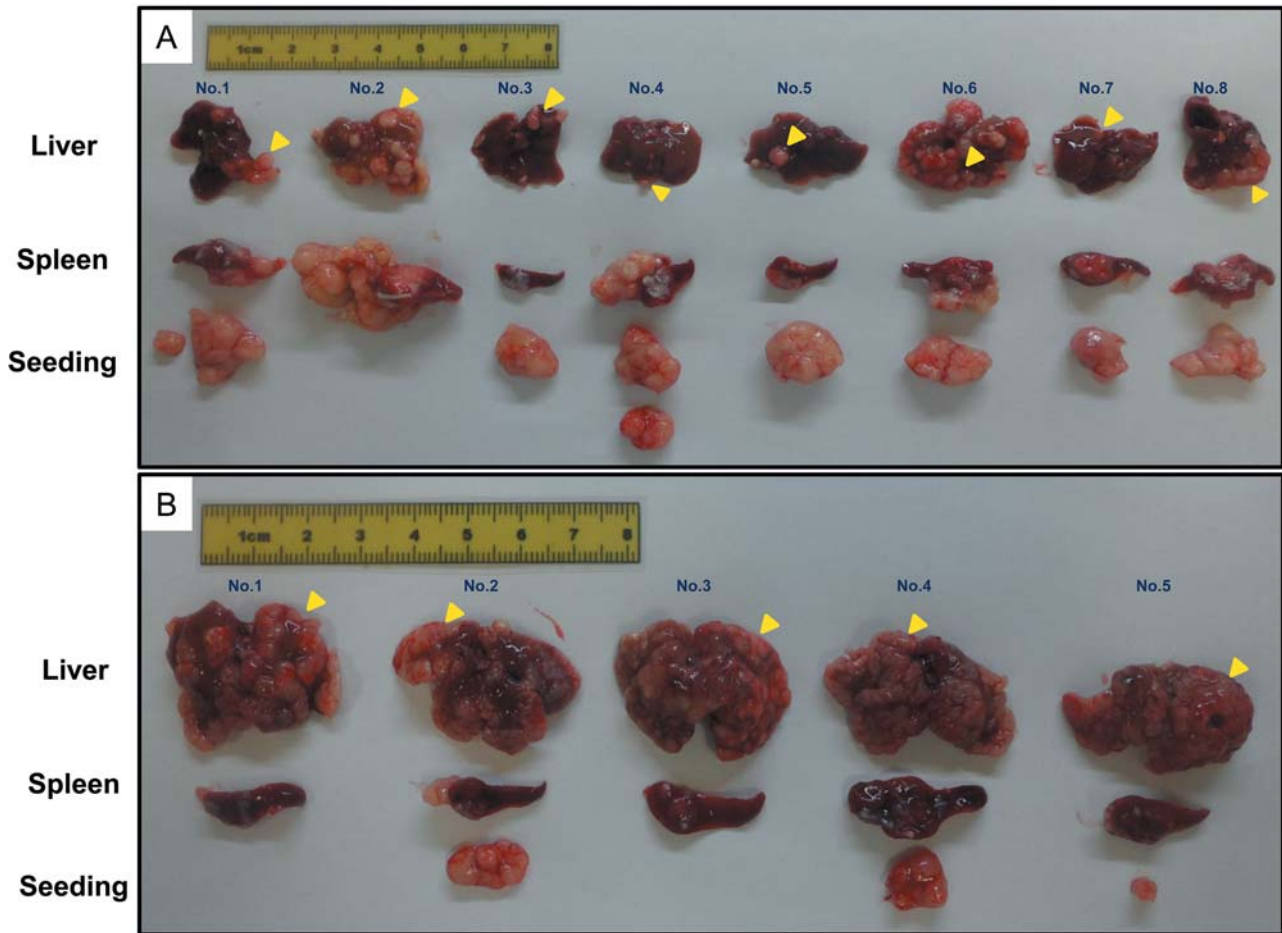


Figure 1. Primary tumor, peritoneal seeding, and liver metastasis in the intra-splenic injection group (A) 2×10^6 cells/injection group, (B) 5×10^6 cells/injection group. Yellow arrows indicate tumor formation in the liver. The first row is the livers, the second is the tumors at the primary sites, and the third is peritoneal seeding.

7 Days after injection

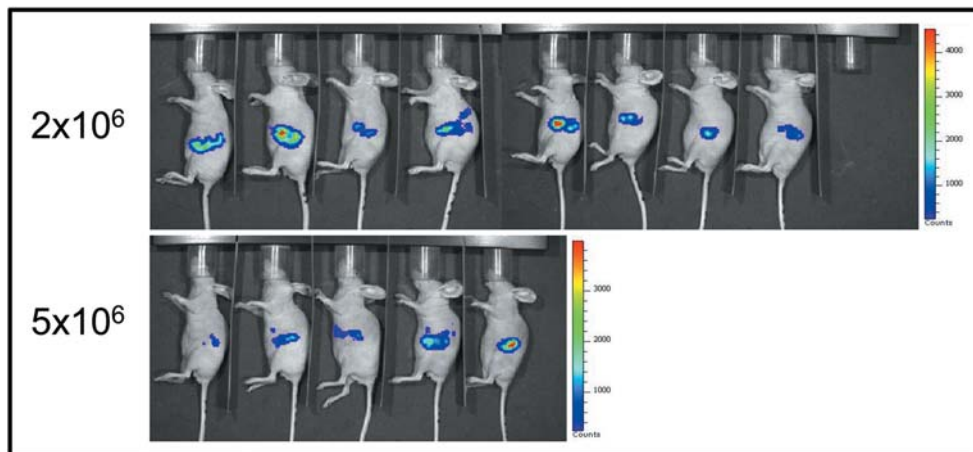


Figure 2. In Vivo Imaging System (IVIS) imaging of the low (2×10^6) and high (5×10^6) cell intra-splenic injected group 7 days after injection. The tumor is shown in color. The densest part of the tumor is shown in red to yellow to green and blue.

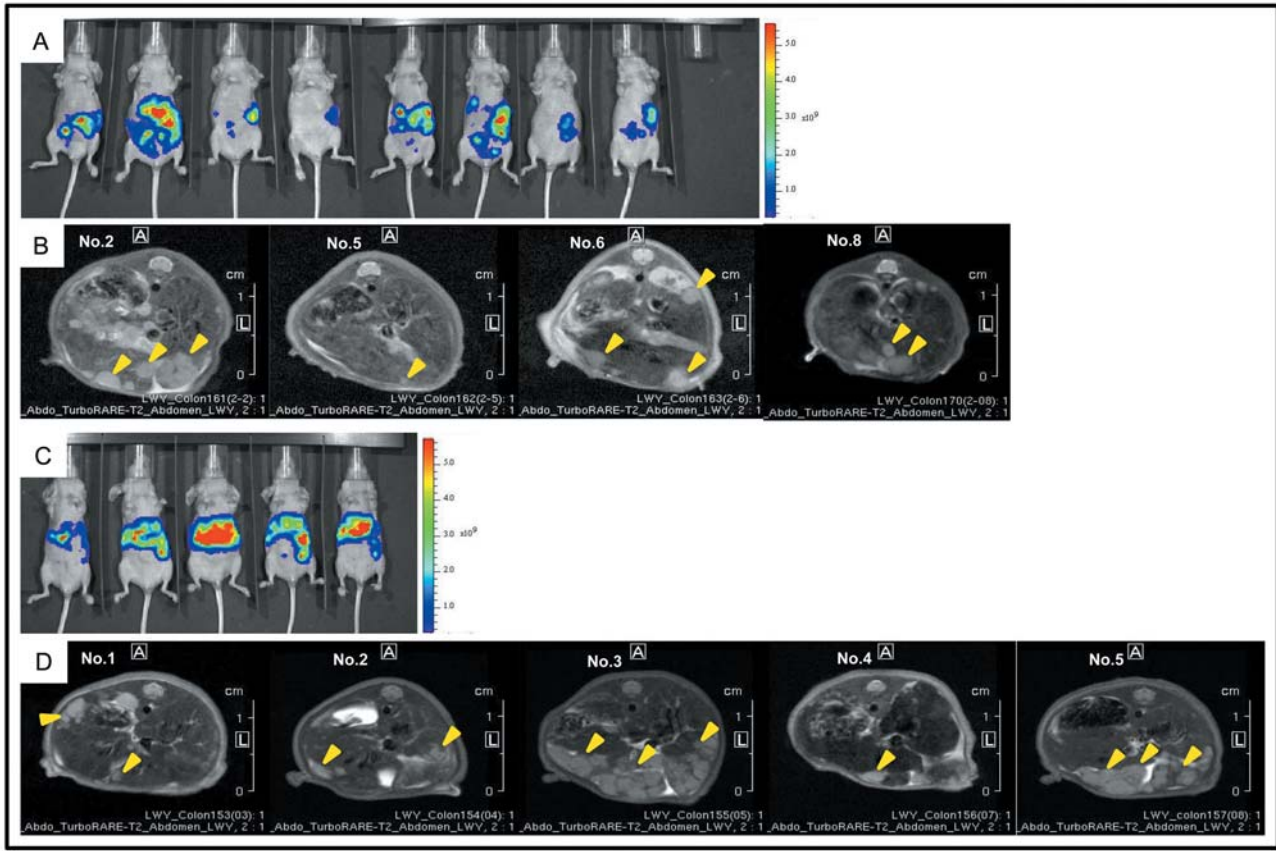


Figure 3. *In Vivo Imaging System (IVIS) (A) and magnetic resonance imaging (MRI) (B) of the low (2×10^6)-cell number intra-splenic injection group 25 days after the injection. IVIS imaging (C) and MRI (D) of the high (5×10^6) cell number intra-splenic injection group 14 days after the injection.*

Table I. *Tumorigenesis rate from intra-splenic injections.*

Group	Cells	Mice	Optical Imaging	Survival days	Take rate	Dissemination site		
						Lymphatic	Hepatic	Seeding
I	2×10^6	8	D7 (1wk)	D37 (6wks)	8/8	5/8 (62.5%)	8/8 (100%)	7/8 (87.5%)
II	5×10^6	5*	D5 (1wk)	D26 (4wks)	5/5	0/5	5/5 (100%)	3/5 (60%)

*Three out of eight animals were dead within 7 days.

Table II. *Tumorigenesis rates from cecal injections.*

Group	Cells	Mice	Optical Imaging	Survival days	Take rate	Dissemination site		
						Lymphatic	Hepatic	Seeding
I	2×10^6	8	D7 (1wk)	D31 (5wks)	7/8	3/7* (43%)	4/7* (57%)	5/7* (71%)
II	5×10^6	8	D6 (1wk)	D30 (5wks)	8/8	4/8 (50%)	6/8 (75%)	8/8 (100%)

*One out of eight animals was dead 25 days after the injection date because of heavy tumor formation.

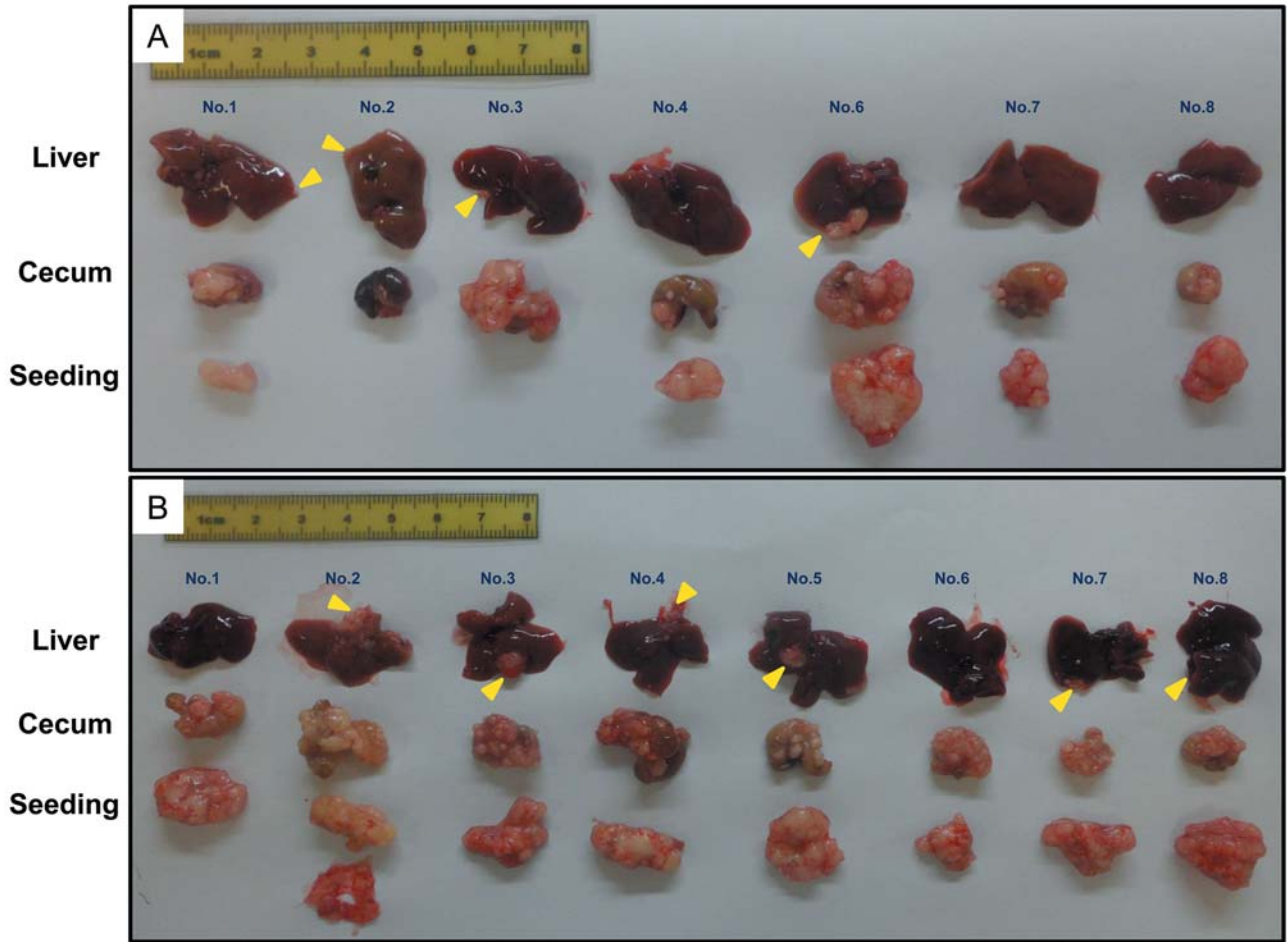


Figure 4. Primary tumor, peritoneal seeding, and liver metastasis of the cecal injection group (A) 2×10^6 cells/injection group, (B) 5×10^6 cells/injection group. Yellow arrows indicate tumor formation in the liver. The first row includes the livers, the second row the tumor at the primary sites, and the third the peritoneal seeding.

15 Days after injection

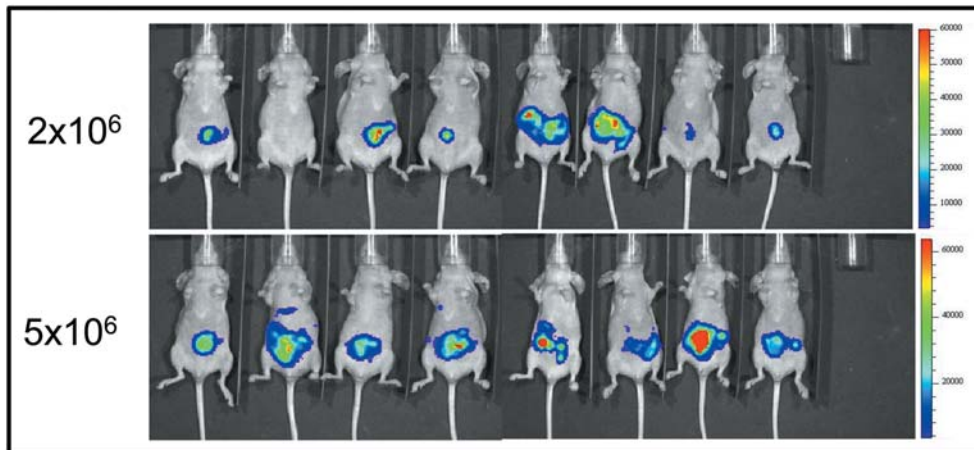


Figure 5. In Vivo Imaging System (IVIS) imaging of the low (2×10^6) and high (5×10^6) cells number cecal injection group 15 days after the injection. In the image, the tumor is shown in color. The densest part of the tumor is shown in red to yellow to green and blue.

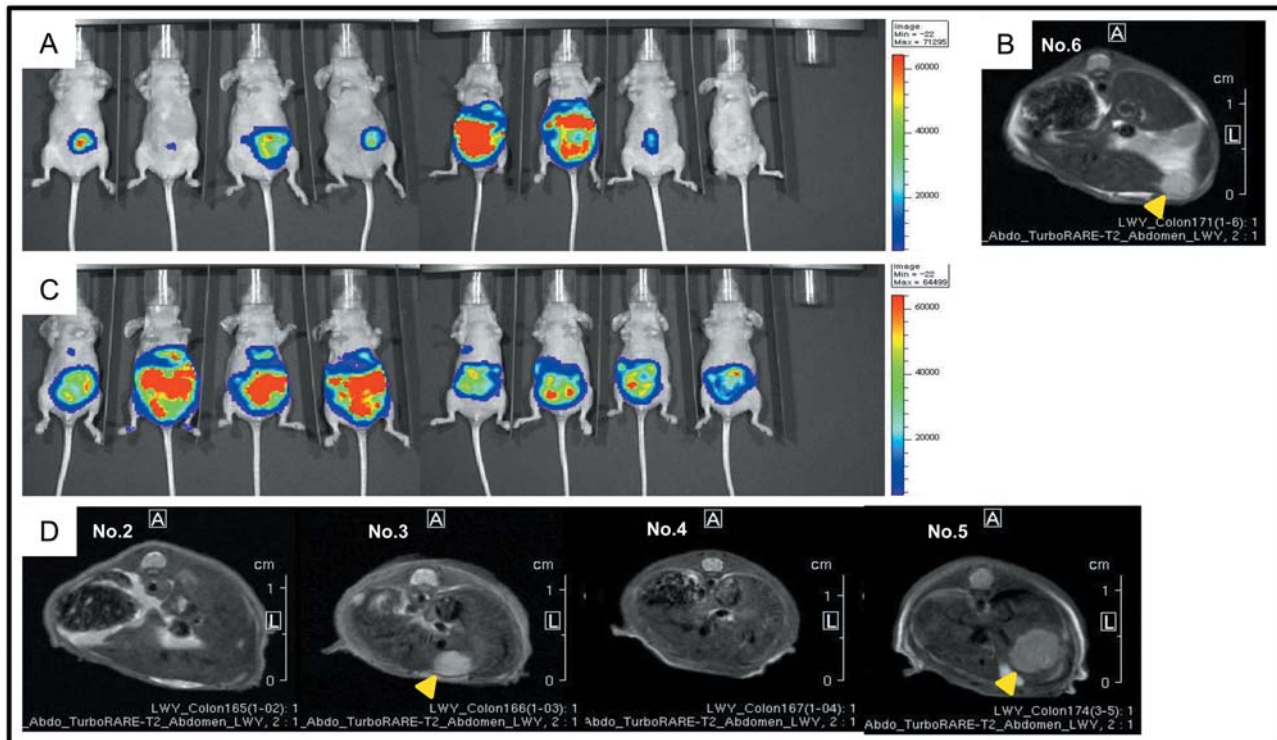


Figure 6. *In Vivo* Imaging System (IVIS) imaging 25 days after injection (A) and magnetic resonance imaging (MRI) 32 days after injection (B) in the low (2×10^6)-cell number cecal injection group. IVIS imaging (C) and MRI (D) in the high (5×10^6)-cell number cecal injection group 25 days after the injection.

Discussion

Metastasis is one of the most important subjects in cancer. In cases of CRC the survival rate decreases once a patient develops metastasis. Several studies have established and characterized metastatic animal models, which is essential for analyzing the mechanism of cancer metastasis and developing new therapeutics (13). Spontaneous and experimental metastatic models are two common methods to establish metastatic tumors in an animal model. In the spontaneous metastatic model the animal is inoculated with cancer cells into specific tissue sites resulting in the formation of a primary tumor that spontaneously metastasizes. The experimental method bypasses the steps of primary tumor growth and intravasation by direct injection into the vasculature, which results in the formation of metastases. Both methods have contributed to our understanding of metastasis, although their relevance to the biology of the multi-step metastatic process should be interpreted with caution.

In the present study, we developed an orthotopic liver metastasis mouse model of experimental and spontaneous liver metastases using intra-splenic and cecal injections with low and high numbers of cells. The results showed that the

cell number and injection site were important factors to develop the *in vivo* liver metastasis model. Intra-splenic injection with a high cell number achieved rapid tumor formation and the highest metastatic rate. However, survival was shorter compared to the other groups. Spontaneous metastasis in the high-cell number group formed a primary tumor and liver metastasis. From a technical aspect, the cecal injection was more difficult and had risks of tumor cell leakage post-injection and intraluminal injection. Historical models of splenic injection do not allow for study of invasion at the primary site for tumor growth, whereas models of cecal injection offer an improvement, as invasion at the injection site can be obtained (14). In the present study, both the splenic- and cecal-injected groups showed invasion at the primary and liver metastatic sites (Figure 7).

The two techniques used to establish the orthotopic mouse model in this study have unique advantages and disadvantages that should be considered depending on the specific experimental aim. The intra-splenic injection model displayed the fastest approach to develop a liver metastasis mouse model. A low cell number (2×10^6) should be used for this model because of the high mortality rate in the high cell number injected group. The cecal injection mouse model represents the process of metastasis from growth of the

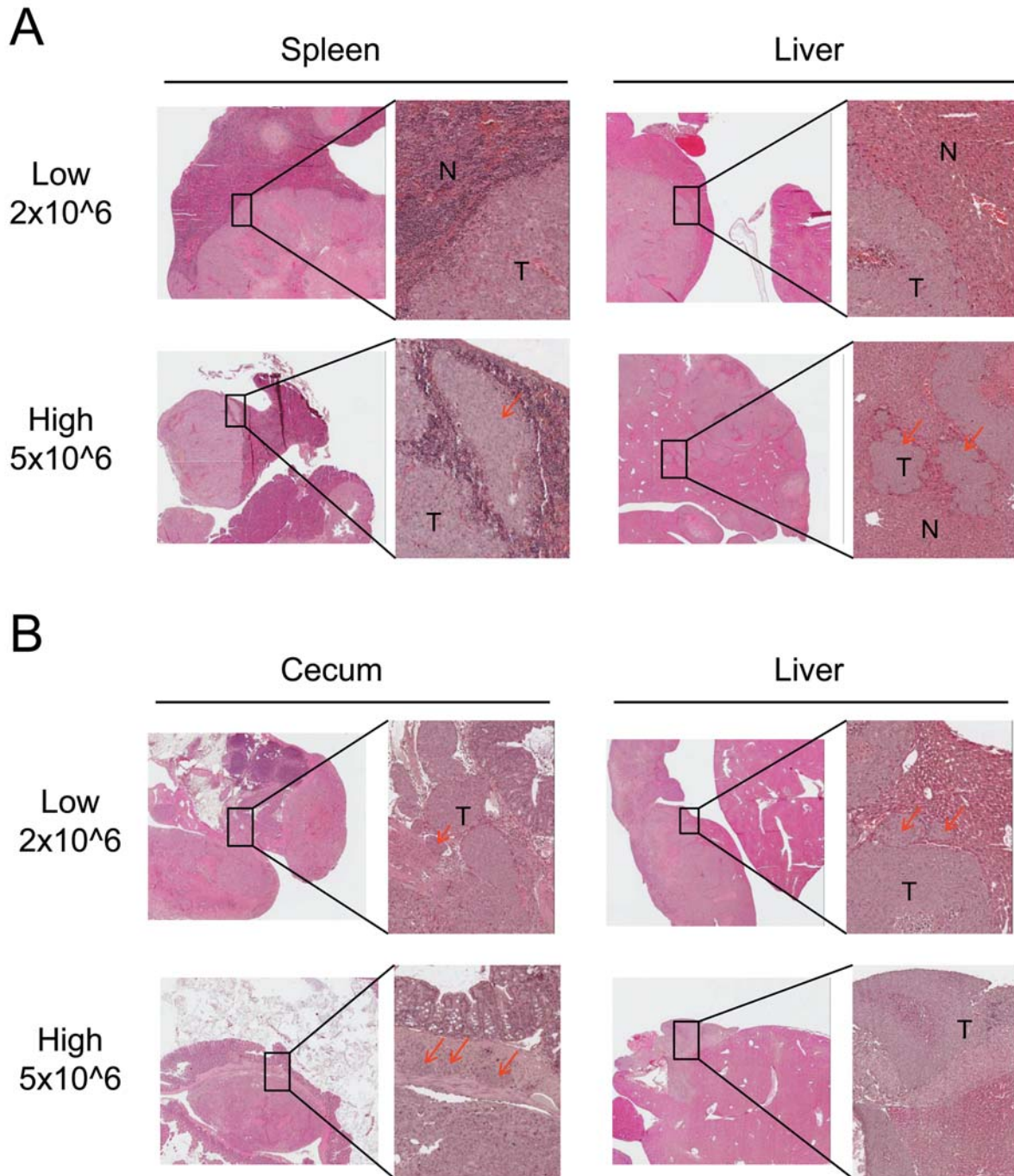


Figure 7. (A) Hematoxylin and eosin (H&E) staining of no.5 in the 2×10^6 cell intra-splenic injection group and no.2 in the 5×10^6 cell group; (B) H&E staining of no.6 in 2×10^6 cell cecal injection group and no.2 in the 5×10^6 cell group. T, Tumor; N, normal cells. Yellow arrows indicate invasiveness of the primary tumor. Left panel, magnification $\times 40$; right panel, magnification $\times 200$.

primary tumor to formation of clinically relevant metastasis. The cecal injection model with high cell number (5×10^6) showed more uniform results for spontaneous metastasis. Moreover, the use of MRI and optical imaging enabled

superior visualization of the entire process of metastasis during early and late colon cancer. Liver metastasis was more easily detected with IVIS imaging than MRI at the early stages. The orthotopic model of colon cancer described

in this study offers a more optimized liver metastasis model for pre-clinical therapeutic evaluations and provides a powerful tool for molecular and cellular characterization of multistep metastasis. Furthermore, the ability to perform MRI and IVIS optical imaging with this model allows for the assessment of tumor spread in real-time in each animal.

Acknowledgements

This study was supported by a grant of the Korea Health Technology R&D project, through the Korea Health Industry Development Institute (KHIDI), funded by Ministry of the Health & Welfare, Republic of Korea (HI09C1552). The authors thank the Center for Molecular and Cellular Imaging (CMCI) for kind technical support with the IVIS and MRI imaging.

References

- 1 Center MM, Jemal A and Ward E: International trends in colorectal cancer incidence rates. *Cancer Epidemiol Biomarkers Prev* 18: 1688-1694, 2009.
- 2 Jemal A, Bray F, Center MM, Ferlay J, Ward E and Forman D: Global cancer statistics. *CA Cancer J Clin* 61: 69-90, 2011.
- 3 Morton CL and Houghton PJ: Establishment of human tumor xenografts in immunodeficient mice. *Nat Protoc* 2: 247-250, 2007.
- 4 Vermaat JS, Nijman IJ, Koudijs MJ, Gerritse FL, Scherer SJ, Mokry M, Roessingh WM, Lansu N, de Bruijn E, van Hillegersberg R, van Diest PJ, Cuppen E and Voest EE: Primary colorectal cancers and their subsequent hepatic metastases are genetically different: implications for selection of patients for targeted treatment. *Clin Cancer Res* 18: 688-699, 2012.
- 5 Sun FX, Sasson AR, Jiang P, An Z, Gamagami R, Li L, Moossa AR and Hoffman RM: An ultra-metastatic model of human colon cancer in nude mice. *Clin Exp Metastasis* 17: 41-48, 1999.
- 6 Yang J, Shikata N, Mizuoka H and Tsubura A: Colon carcinogenesis in shrews by intrarectal infusion of N-methyl-N-nitrosourea. *Cancer Lett* 110: 105-112, 1996.
- 7 Edelmann W, Yang K, Kuraguchi M, Heyer J, Lia M, Kneitz B, Fan K, Brown AM, Lipkin M and Kucherlapati R: Tumorigenesis in Mlh1 and Mlh1/Apc1638N mutant mice. *Cancer Res* 59: 1301-1307, 1999.
- 8 de Wind N, Dekker M, van Rossum A, van der Valk M and te Riele H: Mouse models for hereditary nonpolyposis colorectal cancer. *Cancer Res* 58: 248-255, 1998.
- 9 Fodde R, Edelmann W, Yang K, van Leeuwen C, Carlson C, Renault B, Breukel C, Alt E, Lipkin M and Khan PM: A targeted chain-termination mutation in the mouse Apc gene results in multiple intestinal tumors. *Proc Natl Acad Sci USA* 91: 8969-8973, 1994.
- 10 Heijstek MW, Kranenburg O and Borel Rinkes IH: Mouse models of colorectal cancer and liver metastases. *Dig Surg* 22: 16-25, 2005.
- 11 Fu X, Herrera H, Kubota T and Hoffman RM: Extensive liver metastasis from human colon cancer in nude and scid mice after orthotopic onplantation of histologically-intact human colon carcinoma tissue. *Anticancer Res* 12: 1395-1397, 1992.
- 12 Pocard M, Tsukui H, Salmon RJ, Dutrillaux B and Poupon MF: Efficiency of orthotopic xenograft models for human colon cancers. *In Vivo* 10: 463-469, 1996.
- 13 Francia G, Cruz-Munoz W, Man S, Xu P and Kerbel RS: Mouse models of advanced spontaneous metastasis for experimental therapeutics. *Nat Rev Cancer* 11: 135-141, 2011.
- 14 Rajput A, Dominguez San Martin I, Rose R, Beko A, Levea C, Sharratt E, Mazurchuk R, Hoffman RM, Brattain MG and Wang J: Characterization of HCT116 human colon cancer cells in an orthotopic model. *J Surg Res* 147: 276-281, 2008.

Received March 25, 2014

Revised May 26, 2014

Accepted May 27, 2014